

Centro Nacional de Metrología, CENAM

Report to the 18th meeting of the Consultative Committee for Time and Frequency (CCTF)

June 2009

This brief report describes the main time and frequency metrology activities done at the Centro Nacional de Metrología, CENAM, of Mexico. Taking into account that this report is the first that CENAM submits to the CCTF, main results reported on this document could include a resume of some data older than two years, like data of the UTC(CNM) or data about primary frequency standards development.

1. The UTC(CNM)

1.1 UTC(CNM) generation

The Coordinated Universal Time scale of the Centro Nacional de Metrología (CENAM), UTC(CNM), has been generated since 50143 MJD (March 1996) [1] with no interruptions and since 53000 MJD the $|UTC - UTC(CNM)|$ time differences were smaller than 50 ns during more than 90% of the time. When these time differences were bigger than 50 ns they were also smaller than 80 ns (see Figure 1). During the time interval from 53000 MJD to 54554 MJD the time stability of the UTC(CNM) was 4.3 ns for 5 days and 30 ns for 1 year. Since 50143 MJD the UTC(CNM) has been generated by the 1 pps output of a single Cs high performance clock, referred as Master Clock, from a set of at least 4 Cs clocks. More recently, the CENAM Time and Frequency Division has developed and implemented a time scale algorithm in order to make an efficient use of its ensemble of atomic clocks and then improve UTC(CNM) characteristics of stability, accuracy, reliability and robustness. The preliminary results of such averaged time scale are briefly presented on section 1.3 of this report. The graph below shows the time differences between the UTC and the UTC(CNM) published on the Circular T of the BIPM from 52999 MJD (December 26th, 2003) to 54919 MJD (March 29th, 2009).

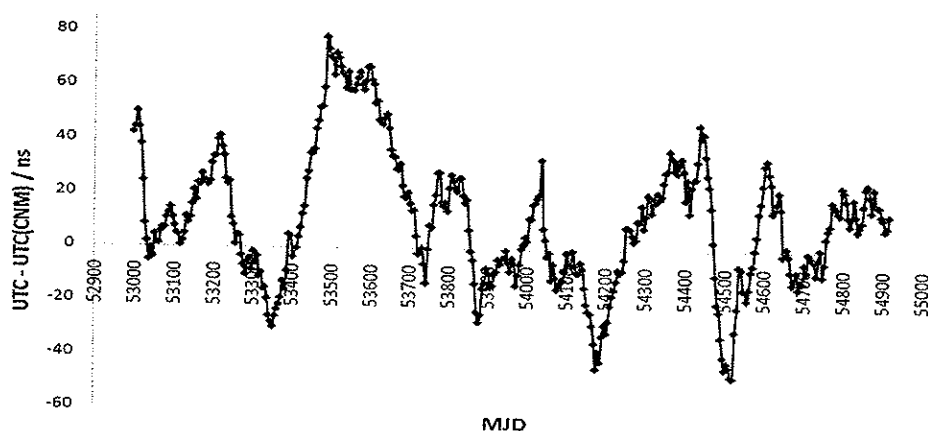


Figure 1. UTC – UTC(CNM) differences as published in the Circular T of the BIPM from 52999 MJD (December 26th, 2003) to 54919 MJD (March 29th, 2009).

1.2 New scheme of the UTC(CNM) generation

The CENAM Time and Frequency Division has developed and implemented a time scale algorithm in order to give better characteristics of stability, accuracy and robustness to the UTC(CNM). With the new method to generate the UTC(CNM), time differences $|\text{UTC}-\text{UTC}(\text{CNM})|$ no bigger than 25 ns, a time stability of 2 ns for 5 days and 15 ns for one year, are expected. In this report we present preliminary results when the time scale algorithm is implemented on four industrial Cs clocks (two of them high performance clocks) and one active Hydrogen maser. The time scale algorithm developed at CENAM is similar to the first presented by NIST as AT1 [2]. However, the way we select the weighting scheme in our algorithm is by $\propto \frac{1}{\sigma}$ and not by $\propto \frac{1}{\sigma^2}$, with the aim to optimize the stability of the CENAM averaged time scale (TA) in the long term where the RWFM is the dominant noise. A complete report of the CENAM time scale algorithm and preliminary results can be found at [3]. The TA time scale is generated since January 2008 and is expected that by the end of the 2009 year the UTC(CNM) will be generated in terms of the TA time scale and not longer with a single Cs clock. In figure 2 we present preliminary results of the frequency stability of the TA scale and in Figure 3 we show the way weighting changes as function of time when the algorithm is implemented on four industrial Cs frequency standards and one active Hydrogen maser. The Cs clocks are referred as CsG (standard performance), CsH (high performance), CsI (high performance) and CsJ (standard performance).

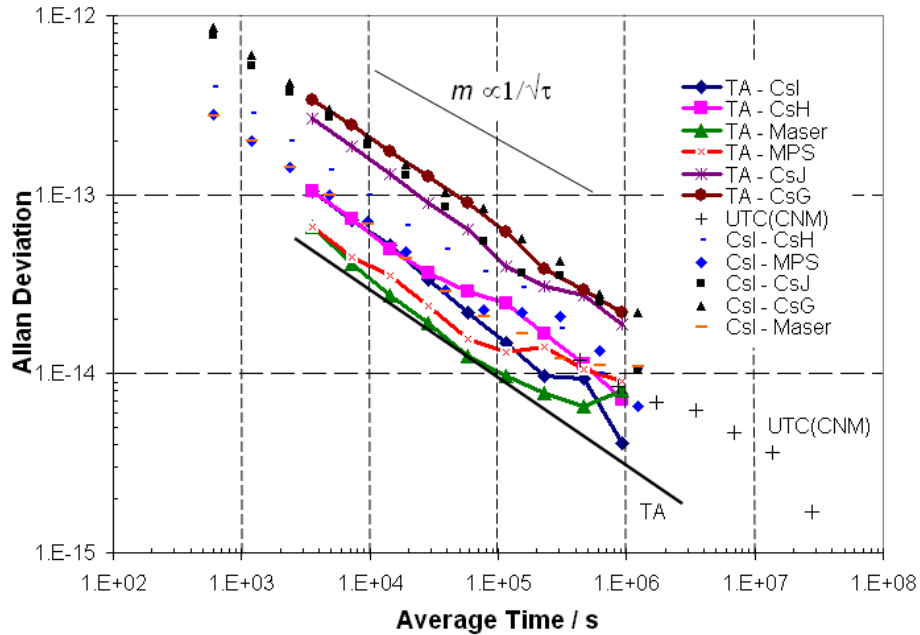


Figure 2. Frequency stability of clocks with respect to the master clock (CsI) and with respect to the TA time scale. The UTC(CNM) stability is also shown according to the BIPM Circular T data. The graph corresponding to the best frequency stability is the estimated TA time scale frequency stability.

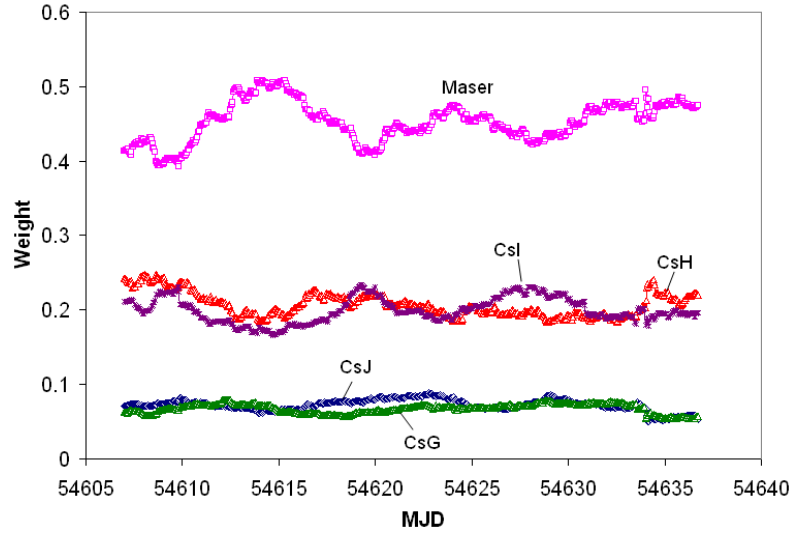


Figure 3. Weight of the participating clocks on the *TA* time scale for a 30 days time period.

2. Development of primary frequency standards

The Centro Nacional de Metrologia, CENAM, has developed a thermal Cesium beam optically pumped frequency standard, CENAM CsOP-1, and is close to complete a cold atoms fountain primary frequency standard, CENAM CsF-1. Evaluation of the major systematic frequency shifts in the CENAM CsOP-1 has been completed [4]. In order to improve its accuracy the linewidth of the central Ramsey fringe has been reduced from 1 kHz to around 250 Hz. The CENAM CsOP-1 is currently under major changes on its Ramsey Cavity and the fractional frequency uncertainty is expected to be in the lower part of the 10^{-14} . On the other hand, DFB diode lasers are used in the optical system of the magneto for trapping, cooling, detection and repumping of the CENAM CsF-1. The MOT is robust against mechanical vibration, acoustic noise and temperature changes in laboratory since DFB diode lasers do not have an extended cavity to reduce its emission linewidth. Characterization of the MOT as a function of several operation parameters such as intensity of beams, beam diameter and gradient of the magnetic field, has been made. Measurement of the number of trapped Cs atoms in our Cs MOT has been reported [5]. Magnetic shielding of the flight region has been designed and built as well as the microwave cavity. Sapphire oscillators have been designed and built [6] to be used as local oscillators for both of the primary frequency standards. Fractional frequency uncertainty on the CENAM CsF-1 clock is expected to be in the lower part of the 10^{-15} .

2.1 Thermal Cesium beam optically pumped primary frequency standard, CENAM CsOP

Since 1998 CENAM started the development of a thermal Cesium beam optically pumped frequency standard named CENAM CsOP-1. Currently this standard is under several important improvements such as: a longer Ramsey cavity, a better magnetic shield system, a more stable C magnetic field, a better vacuum system, among other improvements in order to minimize the uncertainty components arising from systematic effects. After these main changes the name of the clock has changed from CENAM CsOP-1 to CENAM CsOp-2. For CENAM CsOP-2 it is expected a relative uncertainty of at least 3×10^{-14} .

CENAM CsOP-2 beam Tube

The vacuum tube of the CENAM CsOP-2 consists of a stainless cylindrical chamber which contains various components, such as a Ramsey cavity, magnetic shields, C-field coil, optical regions for pumping and detecting, and two cesium ovens. Some of these parts are shown schematically in figure 4. The Ramsey cavity is fabricated of high-conductivity copper with a drift region length $L = 310$ mm and an interaction region length $l = 24$ mm. The atomic beam passes through 3 mm diameter circular apertures drilled through the cavity ends. The oscillating rf magnetic field is parallel with the static magnetic field (C-field) and both are along the atomic beam direction. At both ends of the solenoid are two correction coils, to ensure the maximum C-magnetic field homogeneity. The C-field is induced by a solenoid supported by a 203 mm diameter cylinder of aluminum, that is inside a threefold mu-metal magnetic shield.

Fluorescence detection is augmented by using a concave reflector and a convergent convex lens in each region (pumping and detection region).

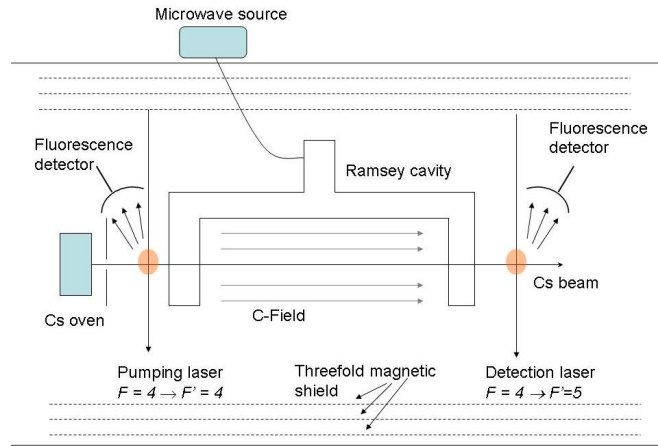


Figure 4. Schematic of the CENAM CsOP-2 beam tube.

The atomic beam and the laser beam interact at the center of the reflector in one side and at the focus of the lens on the other side, so that with the geometry of the components described, the fluorescence efficiency is about 60% supposing an isotropic radiation emission. The light is detected with a photodiode outside the beam tube. A cesium oven is located on each tube end, about 300 mm beyond the cavity end. In normal operation the oven is heated at 380 K and emits an atomic beam through collimator with a circular hole with a diameter of 2 mm.

Table 1. Operational parameter of the CENAM CsOP-2.

Oven temperature	380 K
Drift region length L	310 mm
Interaction length l	24 mm
Mean atomic velocity	215 m/s
Linewidth of microwave transition	300 Hz
C-magnetic field	7.6 μ T

CENAM CsOP-2 laser light Source

In figure 5 is shown the optical arrangement in the CENAM CsOP-2. A DFB high power laser provides the light for pumping and detection (Eagleyard, model EYP-DFB-0852-00150-1500-TOC03-0000), with 150 mW of power, 852 nm wavelength and about 1 MHz linewidth. This laser is frequency stabilized by means of frequency modulation (FM) spectroscopy [7] at the $|6^2 s_{1/2}, F = 4\rangle \rightarrow |6^2 p_{3/2}, F' = 5\rangle$ Cesium transition. The error signal is generated using a frequency modulation of ± 130 kHz at 500 kHz. With the help of a $\frac{1}{2}$ wave plate and a polarized beam splitter, the DFB laser beam is divided in two beams. One beam is used as a detection beam, and the second beam is red shifted 251 MHz using two acousto-optic modulators. Thus, the beam frequency corresponds to the $|6^2 s_{1/2}, F = 4\rangle \rightarrow |6^2 p_{3/2}, F' = 4\rangle$ transition, and it is used as the pumping beam.

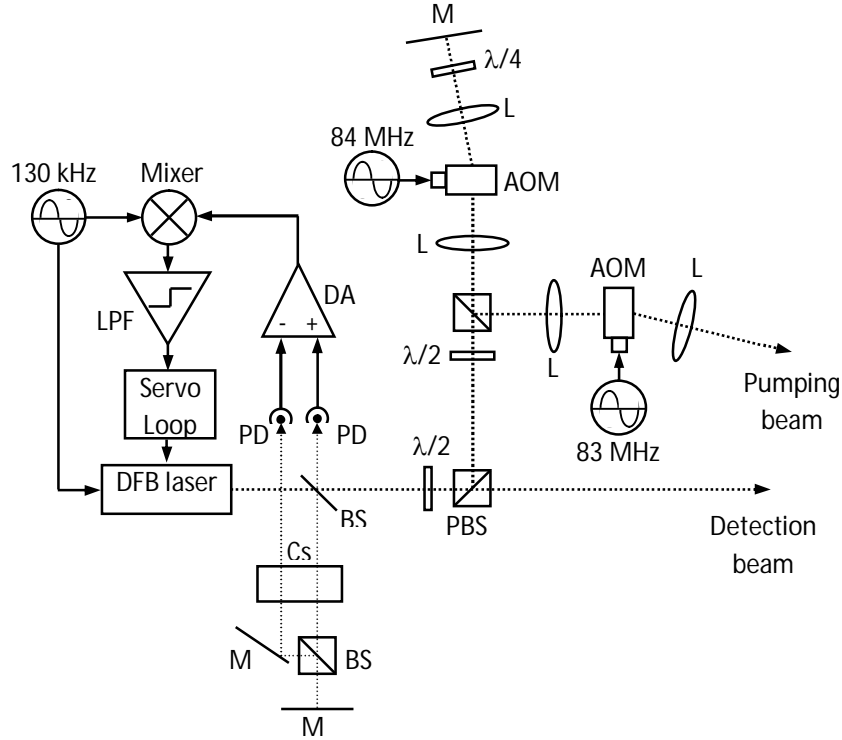


Figure 5. CENAM CsOP-2 optical setup. Where M is a mirror, BS is a beam splitter, PBS is a polarized beam splitter, L is a lens, PD is a photo detector, DA is a differential amplifier, LPF is a low-pass filter, $\lambda/4$ is a $\frac{1}{4}$ wave plate, $\lambda/2$ is a $\frac{1}{2}$ wave plate, and AOM is an acousto-optic modulator.

Experimental results for CENAM CsOP-1 and expected performance of the new CENAM CsOP-2

Figure 6 shows the Zeeman spectrum achieved with CENAM CsOP-1 with a short Ramsey cavity (12 cm long). The full width at half maximum (FWHM) of the Ramsey fringe shown in figure 7 is about 1 kHz. Table 2 shows accuracy evaluation results for CENAM CsOP-1. With the improvements already mentioned from the new CENAM CsOP-2, it is expected that the Ramsey fringe will be reduced about three times, i.e. will be about 250 Hz as shown in figure 9.

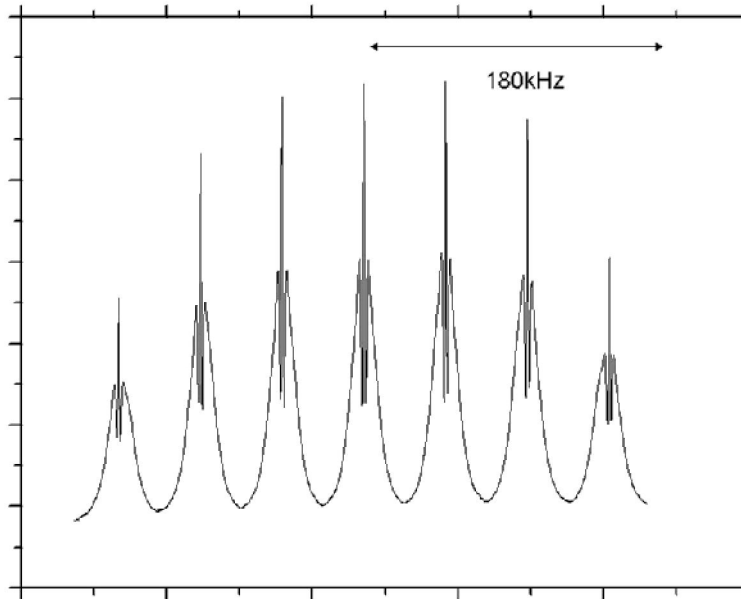


Figure 6. Ramsey fringe of the CENAM CsOP-1 (experimental).

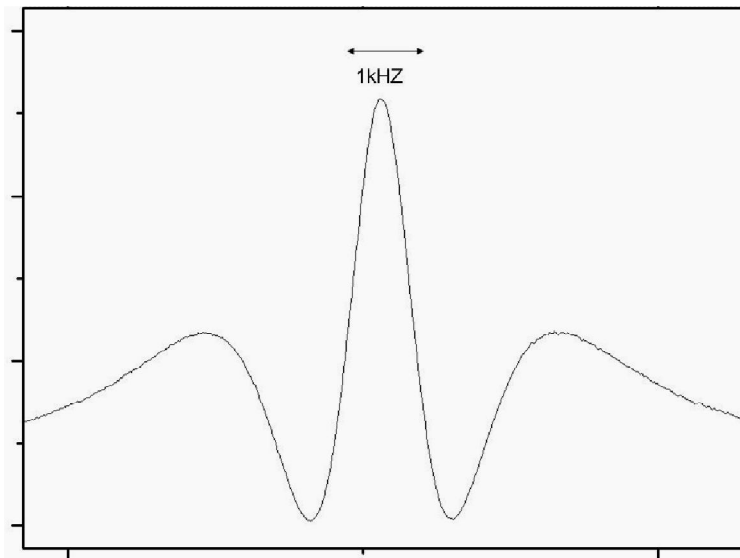


Figure 7. Central Ramsey fringe of the CENAM CsOP-1 (experimental).

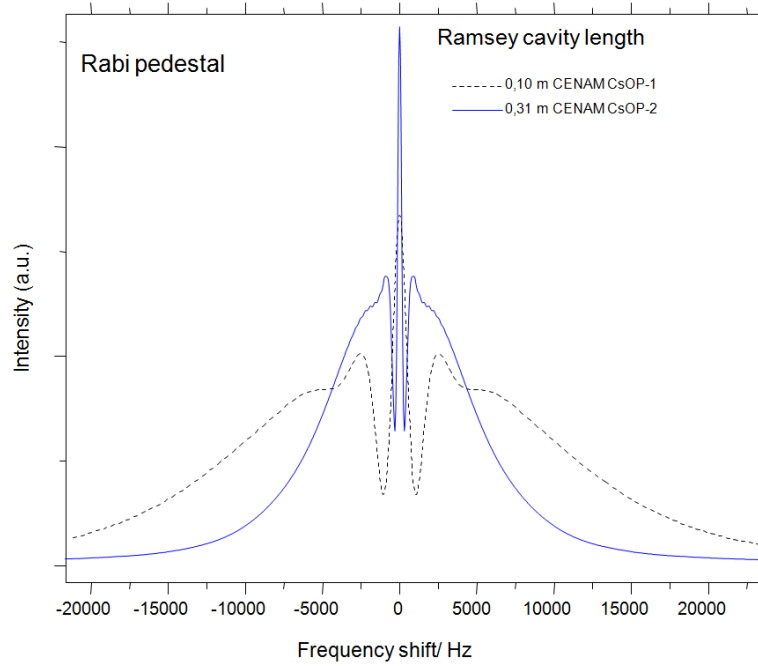


Figure 8. Rabi pedestal comparison between CENAM CsOP-1 and CENAM CsOP-2.

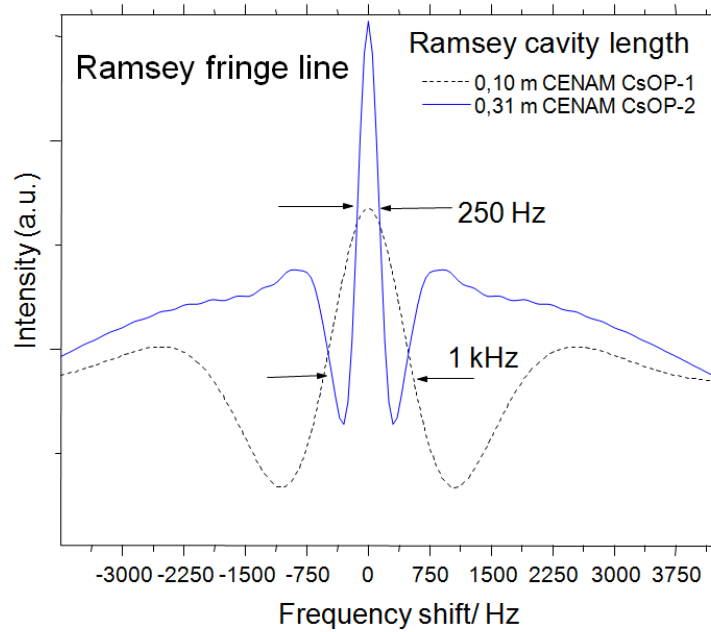


Figure 9. Ramsey fringe line comparison between CENAM CsOP-1 and CENAM CsOP-2.

Table 2. Frequency shifts and their standard uncertainties for the CENAM CsOP-1.

Effect	Shift (10^{-14} Hz)	Uncertainty (10^{-14} Hz)
Second order Zeeman	2915	27
Second order Doppler	-40	5
Blackbody radiation	-1.5	0.1
Gravitation	25.3	0.2
Cavity pulling	32.4	8
End-to End Cavity phase	21	5

2.2 Cs Fountain primary frequency standard, CENAM CsF-1

CENAM CsF-1 MOT

The MOT chamber of the CENAM CsF-1 is made of a stainless steel sphere with twelve ports, six of them are used to feed the laser beams to trap, cold and repump the Cs atoms. The windows of these ports have an anti reflective coating for 852 nm, with a transmission coefficient better than 99 %. An ion pump is used to maintain the Cs pressure around 10^{-6} Pa. The cesium pressure inside the chamber is controlled through a titanium valve and the reservoir's temperature. Figure 10 shows a schematic of the MOT chamber.

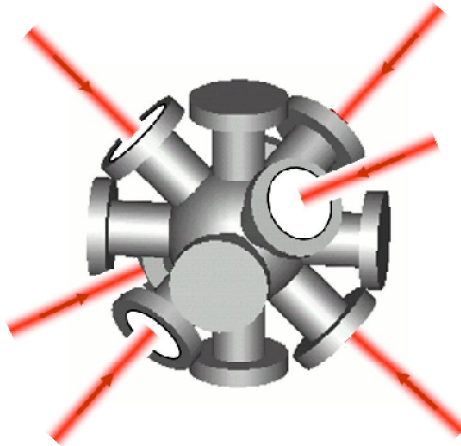


Figure 10. Schematic of the CENAM CsF-1 stainless steel chamber of the MOT.

The magnetic field used to trap the cesium atoms in the centre of the sphere is produced by two coils placed in anti-Helmholtz configuration. The diameter of the coils is 200 mm and the width of the coils is 29 mm with 663 turns each winding. The MOT coils are typically operated at 2 amperes, which induces a gradient of magnetic field of 5×10^{-4} T/cm.

On the other hand, figures 11, 12 and 13 show the setup of the MOT optical system for trapping and cooling, detection and repump, respectively. In total 4 DFB semiconductor lasers are used on the optical part of the CENAM CsF-1. As for trapping and cooling, two semiconductor lasers are used as light sources, named master laser and slave laser. The master laser is a DFB laser diode (Eagleyard, model EYP-DFB-0852-00150-1500-TOC03-0000) with 150 mW output power, 852 nm wavelength (near to the cesium D_2 line), and 1 MHz linewidth. This laser is frequency stabilized at the cooling transition of the cesium using FM saturation spectroscopy. The light from the master laser goes through two acousto-optic modulators in cat's eyes configuration to shift the frequency around 12 MHz to red. In order to increase the power of the cooling laser, a 150 mW DFB laser (slave laser) is stabilized using the light injection method. The slave laser is similar to the master laser. The circular beam of the slave laser is expanded around 4 cm using a lenses arrangement and the beam diameter is controlled by means of a diaphragm. This beam is divided in three beams with 15 mW of power each one. With the purpose of polarize circularly the beams a $\lambda/4$ wave plate is used in each window of the sphere. The re-pumping laser has the same characteristics that the master laser and is stabilized at the $|6^2 s_{1/2}, F = 3\rangle \rightarrow |6^2 p_{3/2}, F' = 4\rangle$ cesium transition. The re-pumping beam is superposed to the cooling beam. The standard geometric arrangement of four horizontal and two verticals beams is used. Because we did not use extended cavity diode lasers, the MOT is highly insensitive to the vibrations.

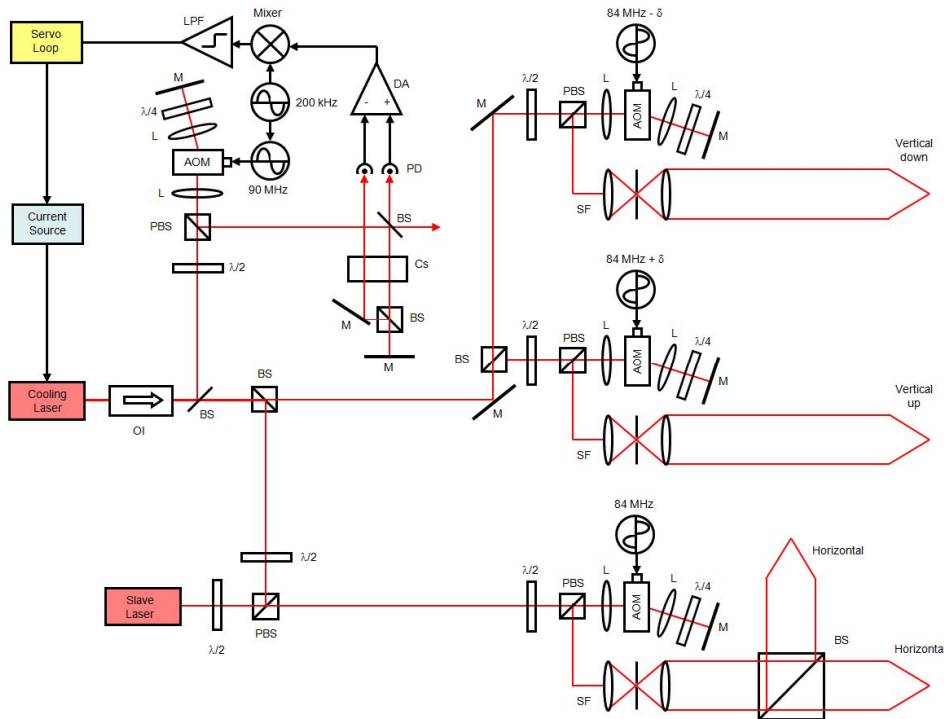


Figure 11. Setup of the cooling and trapping optics of the CENAM CsF-1.

A characterization of the number of trapped atoms in our MOT as a function of several operation parameters such as the intensity of laser beams, the laser beam diameter, the red shift of light, and the gradient of the magnetic field, has been made [5].

Flight region

While writing this report the flight region of the CENAM CsF-1 is currently under development. The threefold magnetic shield has been constructed, which is formed by three μ -metal concentric cylinders, the most internal cylinder has 340 mm in diameter and is 656 cm high. Inside of the magnetic shield is the flight tube. This consists of a cylindrical vacuum chamber, made of copper with 12 cm internal diameter, 13 cm external diameter and 500 mm high. The C field is generated by a coil located outside the flight tube. The diameter of the C field coil is 15 cm. The microwave cavity design is similar to the cavity used at the PTB atomic fountain, CSF1 [8]. It is a cylindrical cavity with a TE₀₁₁ mode in the magnetic field oscillations. This mode exhibits a high intrinsic quality factor, implying a small variation of the field phase with radial position in the cavity. The figure 14 shows a schematic of the CENAM CsF-1 flight region.

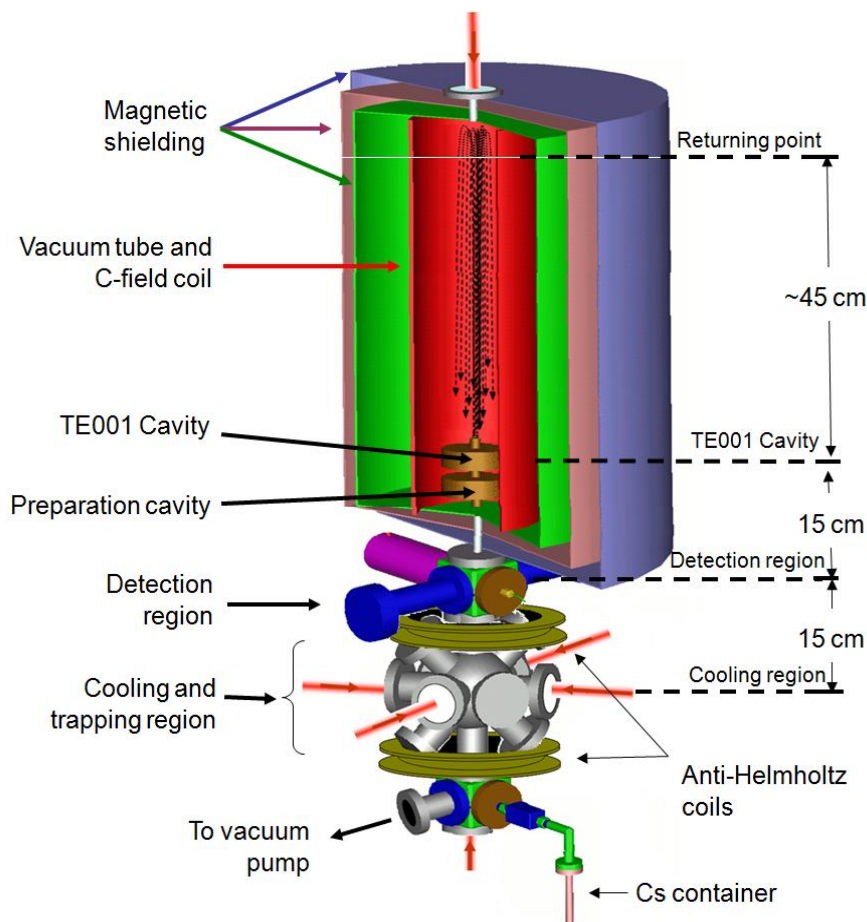


Figure 14. Schematic of the mechanical part of the CENAM fountain clock, CENAM CsF-1.

3. Development of Sapphire crystal oscillators

As local oscillators for the CENAM's primary frequency standards, ultralow phase noise oscillators have been developed using sapphire crystals [6].

3.1. Free-running C-band WGR oscillators

Up to now several free-running sapphire whispering gallery resonator (WGR) oscillators were constructed and tested at CENAM facilities. To design these oscillators, the sapphire WGRs of diameter $D = 69.6$ mm and height $h = 21.5$ mm made of optical quality sapphire have been used. The given WGR dimensions were chosen to be able in perspective to operate the resonator simultaneously at two orthogonal resonant modes $WGH_{7,1,1}$ ($f_{\text{res}} \propto 4.6$ GHz) and $WGE_{15,1,1}$ ($f_{\text{res}} \propto 9.2$ GHz) bearing in mind a possibility of implementation of the dual-mode frequency stabilization system. An unloaded quality factor of the sapphire WGR placed in the cooper cavity proved to be around 250,000 for $WGH_{8,1,1}$ -mode and 300,000 for $WGH_{7,1,1}$ -mode.

In the first constructed free-running oscillators a simple reflection oscillator approach has been implemented. Initially in the designed oscillators the simple open copper cavities were used for sapphire WGR shielding. With the objective to obtain better frequency temperature stability, the oscillator construction has been improved by replacing a cooper cavity with the sealed aluminum cavity suitable to work under a rough vacuum required for a thermal WGR isolation. The WGR was excited on $WGH_{8,1,1}$ -mode having its resonant frequency at 4.98 GHz. In order to achieve a superior phase noise performance, low noise SiGe heterojunction bipolar transistors were chosen as oscillator active devices.

The phase noise spectrum obtained for a beatnote between two identical oscillators is shown in Fig. 13 where can be observe that a beat note phase noise is -133 dBc/Hz at 1 kHz offset frequency. Considering that a single WGR oscillator phase noise is 3 dB lower, we have a final experimental estimation $L(1 \text{ kHz}) = -136 \text{ dBc/Hz}$.

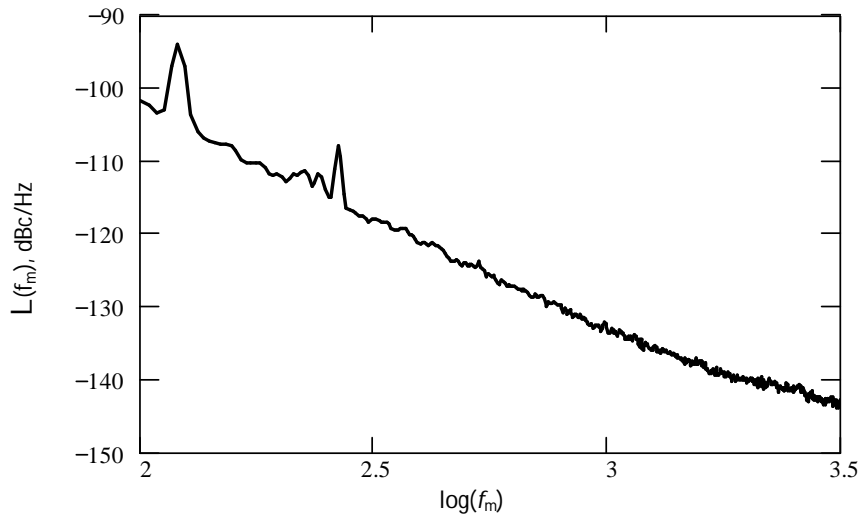


Figure 15. Measured phase noise spectrum of the 1 MHz beat note between 4.79 GHz and 4.80 GHz WGR oscillators.

3.2. WGR oscillator with combined frequency stabilization.

A schematic of the implementation of a Whispery Gallery Resonator (WRG) oscillator is shown in Fig. 16. In the present oscillator configuration a sapphire traveling wave (TW) directional filter is used simultaneously as a feedback resonator in the oscillator loop and as a dispersive element of the frequency discriminator (FD) which together with some additional electronics form an additional phase noise suppression system. In the main oscillator loop we have used a two-stage amplifier built on medium power SiGe HBTs. The designed amplifier allows obtaining about 150 mW power level at the FD input thus achieving a high signal to noise ratio. The entire main oscillator loop electronics including the loop amplifier, a voltage controlled phase shifter and directional couplers have been integrated on a single PCB. Additional electronic blocks needed for a phase noise suppression system including a low noise amplifier (LNA), a phase detector, an electronic phase shifter and an auxiliary amplifier have been combined in a separated microwave module. The designed LNA consists of three amplifying stages and has an overall gain of 33 dB. The first LNA stage as well as the auxiliary amplifier is built on SiGe HBT while in the other two LNA stages commercial SiGe gain blocks are used. The double balanced mixer IC (MACOM MA4EX580-1225T) is utilized as a phase detector. The entire oscillator construction is shown in Fig. 17. In the present design the microwave electronics module assembled in aluminum housing is mounted on the top of the sealed aluminum cavity which incorporates the sapphire WGR.

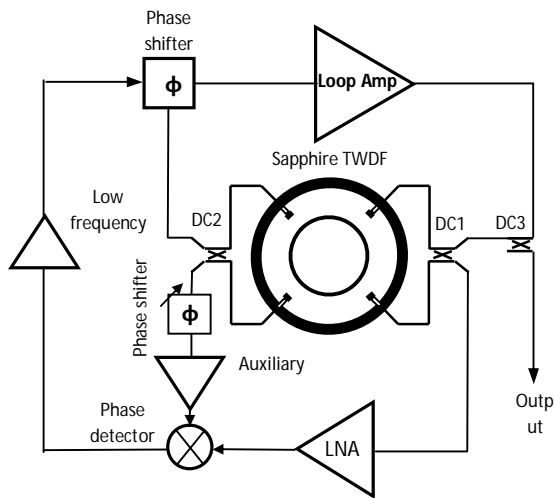


Figure 16. TWDF based microwave oscillator with combined frequency stabilization.



Figure 17. Traveling wave WGR oscillator construction.

A phase noise of the main oscillator loop has been measured analyzing the signal at the phase detector output. According to these measurements at 1 kHz offset, the SSB phase noise resulted to be $L(1 \text{ kHz}) = -124 \text{ dBc/Hz}$. It is expected that once working with the phase noise suppression system the designed oscillator may exhibit a very low phase noise level that could be close to -165 dBc/Hz at 1 kHz offset frequency. In order to accomplish the experimental phase noise characterization a second similar oscillator and a phase noise measurement setup are currently being constructed.

4. Development of optical frequency standards

4.1 Ti:Sa Frequency comb

Since March 2008 CENAM is developing a Ti:Sa frequency comb. A pumping laser of 8 W of 533 nm continuous wave (Verdi) is used for that purpose. Currently some geometries for the Ti:Sa ring have been tested. As preliminary results, pulses with duration time shorter than 100 fs and repetition rate of around 350 MHz have been generated. The frequency comb set up will be slightly modified in order to have light pulses with duration of around 25 fs and repetition rates bigger than 500 MHz. A macrostructure fiber optics will be added in order to expand the comb up to 1 octave. The frequency comb is expected to be completed by the end of the 2009 year.

4.2 Sr lattice clock

Due to the advances during the last decade in reducing the uncertainties on the optical spectroscopy, and also as a chance to contribute to the international community to explore the possibilities to redefine the unit of time of the SI in terms of an optical frequency, CENAM is planning to develop a Sr lattice clock in the near future (within the next 3 years).

References

- [1] BIPM Circular T 100, March 1996.
- [2] M. Weiss and T. Weisser, "AT2, A New Time Scale Algorithm: AT1 plus Frequency variance", *Metrologia* 1991, **28**, pp. 65-74.
- [3] J.M. López-Romero and N Díaz-Muñoz, "Progress in the generation of the UTC(CNM) in terms of a virtual clock", *Metrologia* **45** (2008), S59-S65.
- [4] S. López, M. Lopez, I. Dominguez, and E. de Carlos, "High accuracy evaluation of CENAM's primary frequency standard: Second order Doppler shift" *Proc of the CPEM 2002*, pp. 454-455, 2002.
- [5] M. Talavera O, M. López R., E. de Carlos L., and S. Jiménez S., "Accurate absolute measurement of trapped Cs atoms in a MOT", *Revista Mexicana de Física* **53** (5) 358-365, October 2007.
- [6] N.A. Shtin, J.M. Lopez Romero and E. Prokhorov, "Design and Performance of Ultra Low Phase Noise Reflection Whispering Gallery Resonator Oscillator" *Microwave and Optical Technology Letters*, vol. **49**, no. 8, pp. 2026-2030, 2007.
N.A. Shtin, J.M. López Romero and E. Prokhorov, "Development of ultra low phase noise microwave oscillators at CENAM", *Proc. of the European Frequency and Time Forum 2008*, Toulouse, France, April 2008.
- [7] E. de Carlos López and J.M. López Romero, "Laser frequency stabilization using FM optical pumping spectroscopy", *Revista Mexicana de Física* **54** (3) 222-228, June 2008.
- [8] Schroder, R.; Hubner, U.; Griebisch, D. "Design and realization of the microwave cavity in the PTB caesium atomic fountain clock CSF" *Ultrasonics, Ferroelectrics and Frequency Control*, IEEE Transactions on Volume **49**, Issue 3, March 2002 Page(s):383 – 392.